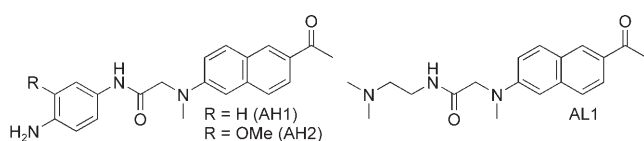


Two-Photon Fluorescent Probes for Acidic Vesicles in Live Cells and Tissue**

Hwan Myung Kim, Myoung Jin An, Jin Hee Hong, Byeong Ha Jeong, Ohyun Kwon, Ju-Yong Hyon, Seok-Cheol Hong, Kyoung J. Lee, and Bong Rae Cho*

We report two-photon (TP) pH probes (AH1, AH2) and a TP lysotracker (AL1, Scheme 1) derived from 2-acetyl-6-(dimethylamino)naphthalene (acedan). These probes can visualize the acidic vesicles in live cells and tissues. Lysosomes and lysosome-related organelles constitute a system of acidic compartments (pH 4.0–5.0) that contain a large number of



Scheme 1. The structures of AH1, AH2, and AL1.

enzymes and secretory proteins exhibiting a variety of functions.^[1,2] To determine their functions, a variety of membrane-permeable fluorescent pH and lysosomal probes have been developed, some of which are commercially available.^[3–5] However, use of these probes with one-photon microscopy (OPM) requires excitation with short-wavelength light (ca. 350–550 nm) that limits their application in deep-tissue imaging, owing to the shallow penetration depth (less than 80 μm) as well as to photobleaching, photodamage, and cellular autofluorescence.^[6] To overcome these problems, it is crucial to use two-photon microscopy (TPM). TPM employs two near-infrared photons for excitation and offers a number

of advantages over OPM, including increased penetration depth (greater than 500 μm), localized excitation, and prolonged observation time.^[7] The extra penetration depth that TPM affords is of particular interest in tissue imaging, because surface preparation artifacts such as damaged cells extend over 70 μm into the tissue interior. However, most of the OP fluorescent probes presently used for TPM have small TP action cross sections ($\Phi\delta$) that limit their usage.^[8] Although a TP pH probe with appreciable $\Phi\delta$ (ca. 42 GM) has been reported,^[4a] the utility of this probe in TPM imaging has not been verified. Therefore, there is a need to develop an efficient TP probe that can visualize acidic vesicles deep inside tissue for a long period of time.

To design an efficient TP probe for acidic vesicles, we chose acedan as the TP fluorophore, because acedan-derived TP probes for Mg^{2+} (AMg1)^[9] and Ca^{2+} (ACa1)^[10] exhibited high photostability as well as significant TP action cross sections for the bright TPM image at low probe concentration, thus allowing the detection of the metal ions deep inside live tissues for over 1100 s. We have introduced an aniline, *o*-methoxy aniline ($\text{p}K_{\text{a}}(\text{BH}^+) \approx 4$), or tertiary amine ($\text{p}K_{\text{a}}(\text{BH}^+) \approx 10$) substituent as the proton-binding site through an amide linkage to the fluorophore. It is expected that AH1 and AH2 would emit TP-excited fluorescence (TPEF) upon protonation at $\text{pH} < 4$, whereas AL1 would emit TPEF in the acidic vesicles, where it should accumulate as the protonated form.^[5] Herein, we report that these probes are capable of imaging the acidic vesicles in live cells and living tissues at greater than 100 μm depth without mistargeting^[9–11] and photobleaching problems. Moreover, AL1 can visualize the transportation of the acidic vesicles in the hippocampal cornu ammonis CA3 region for a long period of time with the use of TPM.

AH1, AH2, and AL1 were prepared in 47–77% yields by reactions of 6-acyl-2-[*N*-methyl-*N*-(carboxymethyl)amino]-naphthalene and a *p*-phenylenediamine derivative or *N,N*-dimethylethylenediamine (see the Supporting Information). The solubilities of AH1, AH2, and AL1 in water are in the range of 5.0–9.0 μM , which are sufficient to stain the cells (Figure S2 in the Supporting Information). The fluorescence spectra of AH1, AH2, and AL1 show gradual bathochromic shifts with solvent polarity (E_{T}^{N}) in the order 1,4-dioxane < DMF < EtOH < H₂O (Figure S1 and Table S1 in the Supporting Information). The large bathochromic shifts with increasing solvent polarity indicate the utility of these molecules as polarity probes.

TP action cross section was determined by investigating the TPEF of the probes using fluorescein as the reference (see the Supporting Information).^[8] The TP action spectra of AH1,

[*] H. M. Kim, M. J. An, Prof. Dr. B. R. Cho
Department of Chemistry, Korea University
1-Anamdong, Seoul, 136-701 (Korea)
Fax: (+82) 2-3290-3544
E-mail: chobr@korea.ac.kr

Dr. J. H. Hong, B. H. Jeong, Prof. Dr. S.-C. Hong, Prof. Dr. K. J. Lee
Department of Physics, Korea University (Korea)

Dr. J. H. Hong, B. H. Jeong, Prof. Dr. K. J. Lee
National Creative Research Initiative Center for Neurodynamics
Korea University (Korea)

J.-Y. Hyon
Biomicsystems Technology Program, Korea University (Korea)

Dr. O. Kwon
Samsung Advanced Institute of Technology (Korea)

[**] This work was supported by a KOSEF grant funded by the Korea Ministry of Science and Technology (MOST) (No. R0A-2007-000-20027-0). J.H.H., B.H.J., and K.J.L. were supported by Creative Research Initiatives of the MOST. S.C.H. and J.-Y.H. were supported by the Seoul R&D program.



Supporting information for this article is available on the WWW under <http://www.angewandte.org> or from the author.

AH2, and AL1 at pH 3.2 indicated a $\Phi\delta$ value of approximately 90 GM at 780 nm, ninefold larger than that of LysoTracker Red (LTR; Figure 1a and Table 1). Thus, TPM images of the samples stained with these probes would be much brighter than those stained with LTR.

When the pH value of the solutions containing AH1 or AH2 was gradually decreased in universal buffer solution (0.1M citric acid, 0.1M KH_2PO_4 , 0.1M $\text{Na}_2\text{B}_4\text{O}_7$, 0.1M Tris, 0.1M KCl), the fluorescence intensity increased dramatically without changing the absorption spectra, probably as a result of protonation blocking the photoinduced electron-transfer

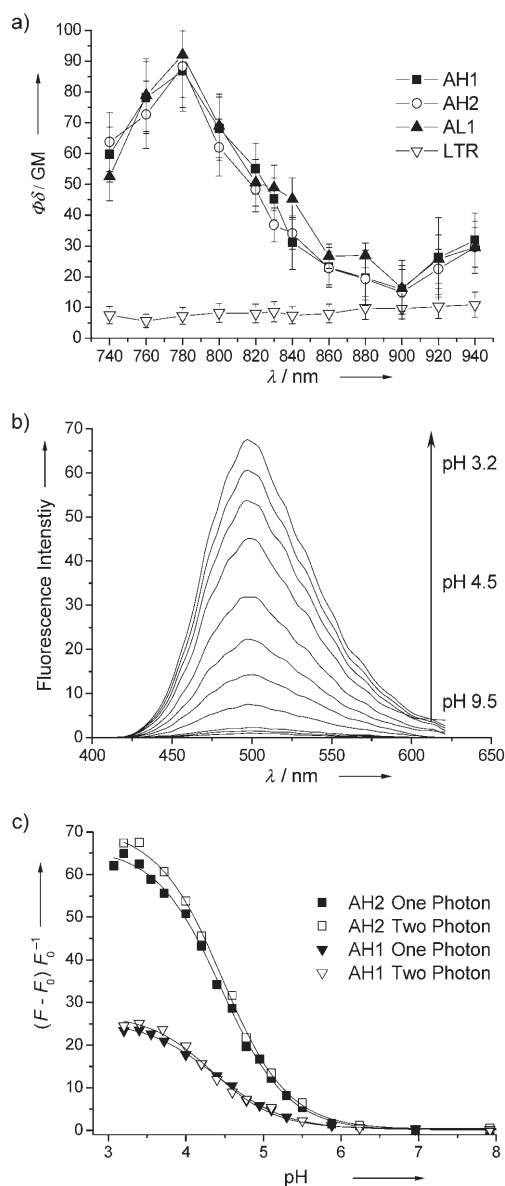


Figure 1. a) Two-photon action spectra of AH1 (■), AH2 (○), AL1 (▲), and LTR (▽) in universal buffer (pH 3.2). b) Two-photon emission spectra of AH2 as a function of pH (3.2–9.5) in universal buffer. c) One- (■, ▼) and two-photon (□, ▽) fluorescence titration curves of AH1 (▼, ▽) and AH2 (■, □) as a function of pH (3.2–8.0). The fluorescence intensity was integrated over the entire wavelength range. The wavelengths for one- and two-photon excitation were 365 and 780 nm, respectively.

Table 1: Photophysical data for AH1, AH2, AL1, and LTR.

Compound	Buffer ^[a]	$\lambda_{\text{max}}^{(1)}/\lambda_{\text{max}}^{\text{fl}}$ ^[b] [nm]	Φ ^[c]	FEF ^[d]	$\text{p}K_{\text{a}}^{\text{OP}}/\text{p}K_{\text{a}}^{\text{TP}}$ ^[e]	$\Phi\delta_{\text{max}}$ ^[f]
AH1	pH 3.2	364/498	0.60	22	4.4/4.5	86
	pH 7.0	365/498	0.03	(26)		nd ^[g]
AH2	pH 3.2	365/496	0.64	64	4.5/4.5	88
	pH 7.0	365/496	0.01	(68)		nd ^[g]
AL1	pH 3.2	364/496	0.72	NA ^[h]	NA ^[h]	92
	pH 7.0	364/496	0.76	NA ^[h]	NA ^[h]	93
LTR	pH 3.2	575/593	0.08	NA ^[h]	NA ^[h]	10

[a] All data were measured in universal buffer (0.1 M citric acid, 0.1 M KH_2PO_4 , 0.1 M $\text{Na}_2\text{B}_4\text{O}_7$, 0.1 M tris(hydroxymethyl)aminomethane (Tris), 0.1 M KCl). [b] λ_{max} of the one-photon absorption and emission spectra. [c] Fluorescence quantum yield $\pm 10\%$. [d] Fluorescence enhancement factor. The numbers in parentheses are FEF values measured by two-photon processes. [e] $\text{p}K_{\text{a}}$ values measured by one- ($\text{p}K_{\text{a}}^{\text{OP}}$) and two-photon ($\text{p}K_{\text{a}}^{\text{TP}}$) processes. [f] Two-photon action cross section. [g] nd = not determined. The two-photon excited fluorescence intensity was too weak to measure the cross section accurately. [h] Not available.

(PET) process (Figure 1b,c and Figure S3 in the Supporting Information).^[3a] The fluorescence enhancement factors $(F-F_{\text{min}})F_{\text{min}}^{-1}$ of AH1/AH2 determined by one- and two-photon processes were 22/64 and 26/68, respectively (Table 1). There is a threefold decrease in the fluorescence quantum yield from AH1 ($\Phi=0.03$) to AH2 ($\Phi=0.01$) at pH 7.0 owing to the *o*-OMe group. Calculations at the B3LYP/6-31G** level revealed that the energies of the highest occupied molecular orbitals (HOMOs) of 4-acetamidoaniline (R1), 4-acetamido-2-methoxyaniline (R2), and acedan are -5.044 , -4.827 , and -5.164 eV, respectively (Figure S6 in the Supporting Information).^[12] Hence, PET from R2 to acedan should occur more efficiently because it is more exothermic. This would predict a smaller fluorescence quantum yield for AH2, as observed. Moreover, the $\text{p}K_{\text{a}}$ values of the conjugate acids of AH1 and AH2 estimated from the fluorescence titration curves are 4.42 ± 0.03 and 4.48 ± 0.02 , respectively, indicating that they are suitable for detecting acidic vesicles with $\text{pH} < 4$ (Figure 1c and Table 1). On the other hand, there was little change in the fluorescence spectra of AL1 with the pH change (Figure S5 in the Supporting Information).

When the macrophages labeled with AH2 and AL1 were repeatedly washed with phenol-red-free Dulbecco's modified Eagle's medium (DMEM), the TPEF intensity decreased gradually, and the change was significantly smaller with AL1 (Figure S8 in the Supporting Information). This result indicates that AH2 is distributed anywhere within the membrane, whereas AL1 exists mostly in the acidic vesicles as AL1H^+ , which does not generally leak out. Thus, AH2 acts as a TP pH probe and AL1 as a TP lysotracker.

To demonstrate the utility of these probes, TPM images were obtained of individual macrophages labeled with 2 μM AH1, AH2, and AL1 (Figure 2). It was previously reported that the TPM images of AMg1- and ACa1-labeled cells emitted TPEF in the 500–620 and 360–460 nm regions, which had been attributed to probes associated with cytosol and membrane, respectively.^[9,10] In contrast, the TPM images of AH2- and AL1-labeled macrophages emitted TPEF only at 500–620 nm (Figure 2b,f) and not at 360–460 nm (Fig-

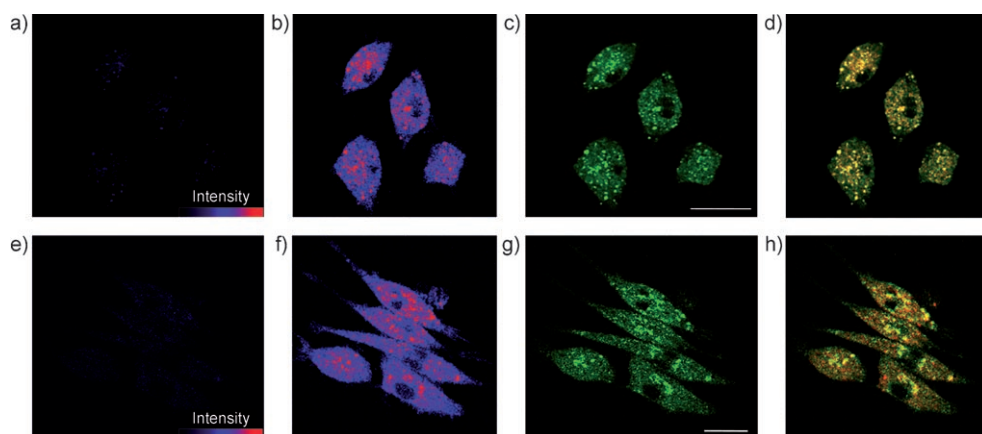


Figure 2. Pseudo-colored TPM images of a, b) AH2- and e, f) AL1-labeled ($2\ \mu\text{m}$) macrophages collected at 360–460 nm (a, e), and 500–620 nm (b, f). c, g) OPM images of LTR-labeled macrophages and d, h) co-localized images. The wavelengths for one- and two-photon excitation were 543 and 780 nm, respectively. Cells shown are representative images from replicate experiments ($n=5$). Scale bars in (c) and (g): $30\ \mu\text{m}$.

ure 2a,e). Moreover, the TPEF spectra of the intense and bright spots in the TPM images of the AH2-labeled cells are almost the same as that of AH2 in the buffer solution with $\lambda_{\text{max}}^{\text{fl}} \approx 500\ \text{nm}$ (Figure S10 in the Supporting Information). A nearly identical result was observed in the TPM images of AH2- and AL1-labeled tissues (Figure S13 in the Supporting Information). These results suggest that the probes are predominantly located in the hydrophilic regions in the cell, presumably because of their low molecular weight. Thus, the acidic vesicles can be detected without interference from the membrane-bound probes.

To unambiguously determine whether the intense (red) spots in Figure 2b are indeed the acidic vesicles, the macrophages were co-stained with AH2 and LTR, a well-known one-photon fluorescent probe for acidic vesicles,^[5] and the TPM image was co-localized with the OPM image. The two images corresponded well (Figure 2d), thus confirming that the bright regions reflect acidic vesicles. Similar results were obtained in the co-localization experiments of AL1 (Figure 2h) and AH1 (Figure S9d in the Supporting Information) with LTR. Hence, these probes are clearly capable of imaging the acidic vesicles in live cells by TPM.

We further investigated the utility of AL1 and AH2 in tissue imaging. The bright-field image of a part of an acute rat hippocampal slice from a 2-day postnatal rat incubated with $10\ \mu\text{M}$ AL1 or AH2 for 30 min at 37°C reveals the CA1 and CA3 regions as well as the dentate gyrus (DG, Figure 3a). The TPM images revealed the acidic vesicles in the same region at 100–250 μm depth (Figure S11 in the Supporting Information), but each image represents the distribution exclusively in the given plane. Since the structure of the brain tissue is known to be inhomogeneous in its entire depth, we have accumulated 40 TPM images at different depths in the range of 100–250 μm to visualize the distribution of acidic vesicles. The accumulated TPM images show that the acidic vesicles are more abundant in CA3 and DG than in the CA1 region (Figure 3b and Figure S12 in the Supporting Information). Moreover, the real-time images reveal rapid transportation of the acidic vesicles between cell body and

axon terminal along the axon (Figure 3c,d and movie S1 in the Supporting Information).^[13,14] Furthermore, the activity of the acidic vesicles could be visualized for more than 1100 s without appreciable decay (Figure S14 in the Supporting Information). This finding underlines the high photostability of this probe in addition to its capability for deep-tissue imaging. Finally, we note that AL1 is superior to AH2 in monitoring vesicle transportation, although both are capable of detecting acidic vesicles deep inside live tissues.

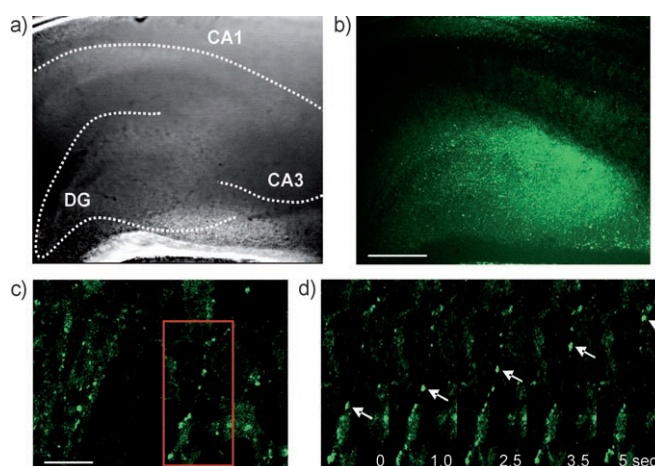


Figure 3. Images of an acute rat hippocampal slice stained with $10\ \mu\text{M}$ AL1. a) Bright-field image showing the CA1 and CA3 regions as well as the dentate gyrus (DG) upon $10\times$ magnification. White dotted lines indicate the pyramidal neuron layer. b) 40 TPM images accumulated along the z direction at a depth of approximately 100–250 μm with $10\times$ magnification to visualize the average distribution of the acidic vesicles in the same regions. c) Image at $100\times$ magnification in CA3 regions at a depth of approximately 120 μm . d) Enlargement of a red box in (c) showing the transport of acidic vesicles along the axon. Scale bars: 300 (b) and $30\ \mu\text{m}$ (c).

To conclude, we have developed TP pH probes (AH1, AH2) and a TP lysotracker (AL1) that can be excited by 780-nm femtosecond laser pulses, easily loaded into the cell and tissue, and which can visualize the acidic vesicles in live cell and tissue by TPM without the artifacts of photobleaching and mistargeting problems. AH1 and AH2 show $\text{p}K_{\text{a}}(\text{BH}^+)$ values of approximately 4.5 and TP fluorescence enhancement factors of 26–68 upon binding with a proton and are suitable for detecting acidic vesicles with $\text{pH} < 4$ at approximately 100–250 μm depth in live tissue. Moreover, AL1 can visualize the transportation of acidic vesicles along the axon

at approximately 120 μm depth for more than 1100 s in live tissue by TPM.

Received: October 4, 2007

Revised: December 27, 2007

Published online: February 13, 2008

Keywords: acidity · fluorescent probes · live tissue · two-photon microscopy · vesicles

-
- [1] S. Kornfeld, I. Mellman, *Annu. Rev. Cell Biol.* **1989**, *5*, 483–525.
- [2] a) E. J. Blott, G. M. Griffiths, *Nat. Rev. Mol. Cell Biol.* **2002**, *3*, 122–131; b) J. Stinchcombe, G. Bossi, G. M. Griffiths, *Science* **2004**, *305*, 55–59.
- [3] a) A. P. de Silva, H. Q. N. Gunaratne, T. Gunnlaugsson, A. J. M. Huxley, C. P. McCoy, J. T. Rademacher, T. E. Rice, *Chem. Rev.* **1997**, *97*, 1515–1566; b) G. Greiner, I. Maier, *J. Chem. Soc. Perkin Trans. 2* **2002**, 1005–1011; c) D. Cui, X. Qian, F. Liu, R. Zhang, *Org. Lett.* **2004**, *6*, 2757–2760.
- [4] a) S. Charier, O. Ruel, J.-B. Baudin, D. Alcor, J.-F. Allemand, A. Meglio, L. Jullien, *Angew. Chem.* **2004**, *116*, 4889–4892; *Angew. Chem. Int. Ed.* **2004**, *43*, 4785–4788; b) F. Galindo, M. I. Burguete, L. Vigarà, S. V. Luis, N. Kabir, J. Gavrilovic, D. A. Russell, *Angew. Chem.* **2005**, *117*, 6662–6666; *Angew. Chem. Int. Ed.* **2005**, *44*, 6504–6508; c) K. M. Sun, C. K. McLaughlin, D. R. Lantero, R. A. Manderville, *J. Am. Chem. Soc.* **2007**, *129*, 1894–1895.
- [5] *A Guide to Fluorescent Probes and Labeling Technologies*, 10th ed. (Ed.: R. P. Haugland), Molecular Probes, Eugene, OR, **2005**.
- [6] a) D. Thomas, S. C. Tovey, T. J. Collins, M. D. Bootman, M. J. Berridge, P. Lipp, *Cell Calcium* **2000**, *28*, 213–223; b) E. Grapengiesser, *Cell Struct. Funct.* **1993**, *18*, 3–17.
- [7] a) W. R. Zipfel, R. M. Williams, W. W. Webb, *Nat. Biotechnol.* **2003**, *21*, 1369–1377; b) F. Helmchen, W. Denk, *Nat. Methods* **2005**, *2*, 932–940.
- [8] C. Xu, W. W. Webb, *J. Opt. Soc. Am. B* **1996**, *13*, 481–491.
- [9] H. M. Kim, C. Jung, B. R. Kim, S.-Y. Jung, J. H. Hong, Y.-G. Ko, K. J. Lee, B. R. Cho, *Angew. Chem.* **2007**, *119*, 3530–3533; *Angew. Chem. Int. Ed.* **2007**, *46*, 3460–3463.
- [10] H. M. Kim, B. R. Kim, J. H. Hong, J.-S. Park, K. J. Lee, B. R. Cho, *Angew. Chem.* **2007**, *119*, 7589–7592; *Angew. Chem. Int. Ed.* **2007**, *46*, 7445–7448.
- [11] C. L. Slayman, V. V. Moussatos, W. W. Webb, *J. Exp. Biol.* **1994**, *196*, 419–438.
- [12] a) A. D. Becke, *J. Chem. Phys.* **1993**, *98*, 5648–5692; b) M. J. Frisch et al., Gaussian 98 (Revision A.7), Gaussian, Inc., Pittsburgh, PA, **1998**.
- [13] a) K. N. Hartman, S. K. Pal, J. Burrone, V. N. Murthy, *Nat. Neurosci.* **2006**, *9*, 642–649; b) J. Burrone, Z. Li, V. N. Murthy, *Nat. Protoc.* **2006**, *1*, 2970–2978.
- [14] a) A. L. Scotti, H. Reuter, *Proc. Natl. Acad. Sci. USA* **2001**, *98*, 3489–3494; b) T. C. Südhof, *Annu. Rev. Neurosci.* **2004**, *27*, 509–547.
-